International Journal of Database Theory and Application
Vol. 11, No.3 (2018), pp. 13-28
hhtp://dx.doi.org/10.14257/ijdta.2018.11.3.02

Hyperspectral Image Classification and Unmixing by using ART and SUnSPI Techniques

Rashmi. P. Karchi[1*] and Nagarajan Munusamy[2]

[1]Department of Computer Science, Bharathiar University, Coimbatore-641046, Tamilnadu, India*
[2]Department of Computer Applications, CMS College of Science and Commerce, Coimbatore - 641 004, Tamilnadu, India
[1]rashmikarchi@gmail.com, [2]mnaagarajan@gmail.com*

Abstract

The Hyperspectral images extract, collect and process the information from across the electromagnetic spectrum. The main aim of the hyperspectral imaging is to get the spectrum from each pixel in the images, to find the objects, materials or detecting processes. The spectral range in the hyperspectral images provides the ability to identify chemical types on the environment of Mars more precisely than before. For extracting the hidden features in the mixed pixel the freshly established hyper spectral image classification techniques are demonstrated. Further proposed method is experimentally calculated by using both pretended and actual hyperspectral datasets. The integration of Unmixing algorithm termed "Sparse Unmixing of Hyperspectral information with Spectral a Priori data" with the Singular Spectrum Analysis approach is employed. To get better result the Clustering is done by "Adaptively Regularized Kernel-Based Fuzzy C-Means" and Segmentation with "Watershed" of images is carried out. Further the ART classifier is employed for better level of classification. The integration of these methods signifies an innovative contribution in the research field of hyperspectral imagery.

Keywords: *Hyperspectral image classification, mixed pixel, Unmixing, Clustering and Segmentation*

1. Introduction

In the past decades the hyper-spectral imaging has been the locale in the active inspection, improvement, and hyper-spectral images have been able merely to researches. The hyper-spectral imaging system has been entered the mainstream of the remote sensing. The hyper-spectral images have found many applications in resource management, mineral exploration, agriculture and environment monitoring. Although valuable utilization of the hyper-spectral images needs full knowledge on the nature and restrictions of facts and the different strategies for the dispensation and understanding. The hyper-spectral images can be captured with the help of acquisition instrument known to be imaging spectrometers. The spectrometer imaging sensors have concerned the convergence of two allied however distinctive technologies: spectroscopy and distant imaging of the Earth and terrestrial surfaces.

The spectroscopy is learning of light that can be produced by or reflected as of resources and its difference in energy by wavelength as shown in Figure 1.

Received (January 14, 2018), Review Result (May 10, 2018), Accepted (May 20, 2018)

ISSN: 2005-4270 IJDTA

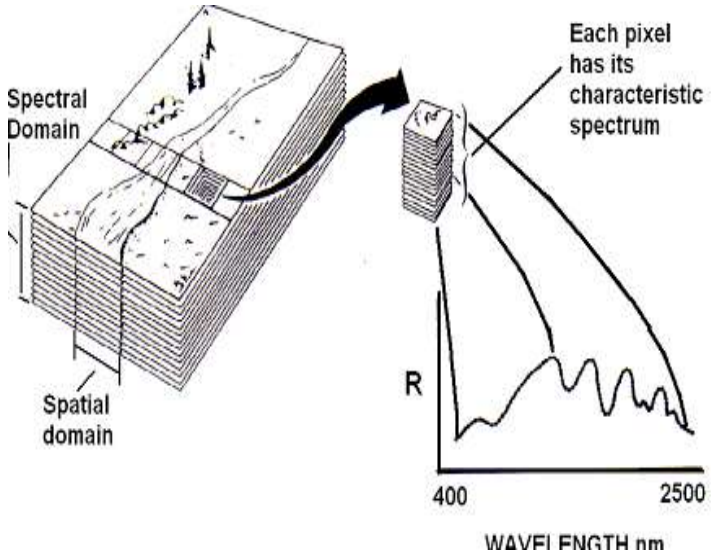

Figure 1. Hyperspectral Imaging with Spectroscopy

In various digital images, sequential dimensions of minute areas can be done in a reliable geometric outline as the sensor stage moves and succeeding dispensation is necessary to gather them into an image. In anticipation of freshly, images are controlled to one or more comparatively broad wavelength bands with restrictions of detector designs with the desires of information storage, transmission, and processing. The advancement in the area of hyper-spectral imaging have approved the plan of images that comprise spectral ranges and resolution equivalent to ground-based spectrometers. In object tracking techniques with the availability of abundance of elevated powered computer, the accessibility of expensive and good quality OMEGA instrument has formed a huge deal of attention in object tracking techniques present in hyper-spectral images.

The OMEGA instrument captures the two dimensional images of Mars. The mixed pixel arises due to inadequate spatial resolution of Hyper-spectral sensors. Several methods have been proposed in the literature for the unmixing of hyper-spectral data and are classified and categorized in statistical, geometrical, and spares regression based approaches. The hyperspectral data processing requires the very large computational resources in terms of computation, storage, and I/O throughputs, particularly when real-time processing is considered. For the sparse unmixing of the hyperspectral images, a novel algorithm called Spares unmixing using spectral a priori information (SUnSPI) is proposed in this paper. This algorithm aims to find the optimal subset of endmembers scene. Lately, as more spectral libraries happen to openly obtainable, it takes the spectral records as a priori knowledge. Since from few decades so many researchers are working to improve the system performance. The referred research paper for the proposed work briefly explained in literature survey.

The rest of the paper is organized into four sections: Section 2 reviews the developments in classification and unmixing of the hyperspectral imagery. The proposed model of hyperspectral image classification and unmixing by using ART and SUnSPI technique is described in Section 3. The experimental results and analysis are given in Section 4. The Section 5 concludes the proposed work.

2. Review of Related Work

The hyper-spectral imaging system has entered the mainstream of the remote sensing. The applications of the hyper-spectral images have found many applications in resources of management, mineral exploration, agriculture and environment monitoring. Some of the research work is carried out by the researchers in the area of hyperspectral image

classification and unmixing and is summarized here. Olivier Eches *et. al.*, [1] have discussed on the new algorithm for the hyper-spectral image unmixing. A Bayesian model is introduced to exploit the correlation. The image is to be unmixed, if supposed to be separated in to classes where the property of abundance coefficient is consistent. A Markov Random Field (MRF) can be projected in the replica for spatial dependence of pixels in any class. Provisionally upon a specified class, every pixel can be modelled by the traditional linear mixing form by additive white Gaussian noise. This scheme can be investigated well known linear mixing form. In this scheme parameter include abundances for every pixel. Further it also includes the variances and means of the abundances for every class and a classification map signifying the classes of every pixel in an image. The accuracy of the proposed methods can be illustrated on synthetic and actual data.

Shaohui Mei *et. al.*, [2] have discussed on the spectral variation that are reflective in distantly intellect images suitable to changeable imaging circumstances. The broad attendance of the spectral difference degrades the presentation of hyper spectral study, such as categorization with spectral unmixing. This low-rank matrix approach can be used to ease spectral difference for the hyper-spectral image study. The hyper-spectral image information is decomposed into the low-rank matrix with the sparse matrix. The intrinsic spectral characteristics are represented by low-rank matrix and spectral difference can be accommodated with sparse matrix. As a result, the presentation of image analysis is enhanced by effective on the low-rank matrix.

Paris V. Giampouras *et. al.*, [3] have described the unmixing of the hyper-spectral data, in which a novel unmixing algorithm are introduced for the improvement of identification of the materials present in the hyper-spectral images. Mainly two unmixing techniques have been proposed in this paper, in an effort to utilize the spatial correlation with sparse representation of pixels are lying in homogeneous areas of hyper-spectral images. The resultant normalized cost purpose is minimizing with a) an incremental proximal sparse with low-rank unmixing algorithm b) the technique based on irregular minimization system of multiplier (ADMM).

Xiong Xu *et. al.*, [4] have presented the various unmixing methods of hyper-spectral images in this paper. The Subpixel mapping algorithms has been extensively exploited to establish the spatial allocation of various land-cover classes in mixed pixels at the subpixel scale with adapting low-resolution fractional abundance maps (approximated by a linear assortment model) into the better classification maps. It has been evident that the exploited abundance map has a strong force on succeeding subpixel mapping process. A detailed quantitative estimation of dissimilar aspect in linear spectral combination study, such criterion employed to decide the kinds of pixels, the profusion sum-to-one restraint in unmixing, and correctness of exploited abundance maps, is examined.

In our previous survey work presented in [5], it is described the summary of the different spectral unmixing models and algorithms with the state-of-the-art technologies employed for the Hyperspectral unmixing of mars dataset captured with several instruments.

The work presented by Sicong Liu *et. al.*, [6] describes a fresh multitemporal spectral unmixing (MSU) method to attend the demanding multiple-change discovery crisis in bi-temporal hyper-spectral images[7-15]. The proposed method gives the spectral-temporal variations at a subpixel level. The measured Change Detection (CD) crisis can be analyzed in a multi-temporal area, where the bitemporal spectral combination forms described to analyze the spectral composition in a pixel. Distinct multi-temporal end members (MT-EMs) can be extracted according to the routine and unverified algorithm. The end member grouping system can be applied to change MT-EMs to notice the sole modify classes. Finally, the measured multiple-change recognition trouble can be solved with analyzing abundances of change and no-change modules and their involvement to every pixel. The detailed description of the proposed methodology is given in the next sections.

3. Proposed Methodology

The description of the steps/ procedure involved in the proposed methodology for the Unmixing and classification of the hyperspectral images is given in the following. The proposed system is divided into two phases namely, Testing and Training phase. Training phase involves learning the cropped Hyperspectral images by extracting features using Singular Spectrum Analysis (SSA) and storing in the knowledge base. In testing phase, the Hyperspectral image is enhanced [16] with pre-processing by using Singular Value Decomposition (SVD) algorithm. The Sparse Unmixing of Hyperspectral Data Using Spectral Priori Information (SUnSPI) is employed for Unmixing Hyperspectral images followed by feature extraction. These features are matched with already stored features in the knowledge base using ART Classifier. The block diagram of proposed system for Unmixing and classification of Hyperspectral image is shown in Figure 2.

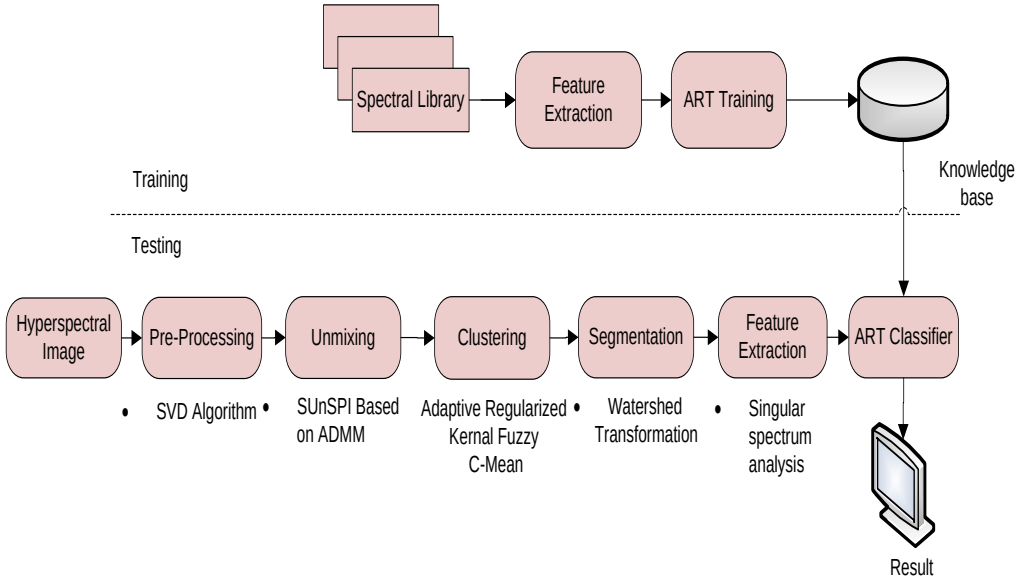

Figure 2. Block Diagram of Proposed System for Unmixing and Classification of Hyperspectral Image

i. Training Phase: In this phase, Hyperspectral images are taken as input image from the spectral library from hyperspectral reflectance dataset. The spectral library consists of iron oxides ranging from 0.9 μm to 1.3 μm, Hydrated Minerals having spectral characteristics at 1.4, 1.9 and 2.5 μm, Surpentines spectra having very strong M shape duet absorptions at the 1.91 am, Olivines spectra having spectral feature at 1 μm and other minerals spectral ranging from 0.2 to 2.02 μm. The materials falling in this spectral range the features are extracted using Singular Spectrum Analysis (SSA) method. These extracted features are trained and stored in knowledge base for further validation.

ii. Testing phase: In testing phase, the Hyperspectral image is taken as an input/test image and these images are pre-processed using the Singular Volume Decomposition algorithm. The size of the Hyperspectral images is reduced and also the significant reduction in complexity is done to facilitate the near real time processing speed. Unmixing of the hyper-spectral image is done using the "Sparse Unmixing of Hyperspectral Data Using Spectral a Priori Information" (SUnSPI) algorithm in which the mixed pixels are analyzed and the materials present in the hyper-spectral images are differentiated for the proper classification. Further, for the better improvement in the classification the clustering of the images is done using the "Adaptively Regularized Kernel-Based Fuzzy C-Means"

(ARKFCM) technique in which cluster images are formed and the standard image is taken for the segmentation [16, 17]. In the segmentation "Watershed segmentation" algorithm is used for the better classification as shown in Figure 2.

The next step is extracting features from these Hyperspectral images of mars dataset using Singular Spectrum Analysis approach. By eliminating noise components in extorting the characteristics, the discerning capability of characteristics will be enhanced significantly. SSA permits many possibilities for presenting considerable possible for mars dataset. An application of SSA approach to each spectral pixel lead to a restoration procedure that enlarges the correctness in classification task for an image hsv000f9c0_01_ra2095_trr3. The main purpose of SSA here is to decay a unique sequence into sub-series and some self-governing mechanism. Consequently, the main competence of SSA are as pursue: Periodicities with varying amplitudes and complex trends, discover the structures in tiny time sequence and envelopes of alternating signals, removal of episodic component, trends and smooth for mars dataset.

The extracted features of mars dataset, which are generated during training phase are compared with the features stored in the knowledge base by using ART classifier. The final results are validated by examining the classification accuracy. Series of real time neural network models are considered as the ART (Adaptive Resonance Theory), which provides both unsupervised and supervised learning [18, 19], prediction, and detection and mainly with pattern recognition for hsv000f9c0_01_ra2095_trr3 mars dataset. The ART classifier is designed for both analog and digital input patterns. Thus in our proposed system the ART classifier for digital input patterns are utilized for better level of classification and recognition rate for Hyperspectral images.

3.1. Unmixing of Hyperspectral Data Using Spectral a Priori Information

Let $A \in R^{L\times m}$ indicate the spectral library, where L represents the amount of the bands, and m represents the amount of spectral signature in library. The linear sparse unmixing form supposes that the experiential range vector of the mixed pixel $y \in R_L$ is a linear arrangement of only the little spectral signature in spectral library as given in equation (1),

$$y = Ax + n \tag{1}$$

In the SUnSPI model, the assumption is made that a few resources in spectral library is recognized to be real in hyper-spectral scene. Assume $S=\{1,\ldots,m\}$ is the set of the indices of every spectral signature in spectral library, $P \subset S$ represents the position of the indices equivalent to resources that known to be real in scene, and $S/P=\{x \in S/x \notin P\}$ represents the set dissimilarity of and P. Let X_P indicate the rows of the X that contain the indices as of the set P. To integrate the ethereal apriori data into the sparse unmixing form, we must assure that spectral signature indexed with P is active in representation of the hyper-spectral facts. The other spectral signature may possibly or may not be energetic, however only a few of them must be vigorous due to subspace personality of hyper-spectral information. This pole of analysis leads us to believe enforce the row sparsity of X(S/P) though departure XP only.

$$\min_X \frac{1}{2}\|AX - Y\|_F^2 + \lambda_S \sum_{t=1}^{K}\|x_1\|_1 + \lambda_P \sum_{t\in \frac{S}{P}}\|x^t\|_2 \qquad \text{subject to: } X \geq 0. \tag{2}$$

Here, $\|X\|_1$ and $\|X\|_{2,1}$ to denote $\sum_{t=1}^{K}\|x_1\|_1$ and $\sum_{t=1}^{m}\|x^t\|_2$ respectively $H \in R^{m\times m}$ is a diagonal matrix associated to place P:

$$h_{ii} = \begin{cases} 0, & \text{if } i \in P \\ 1, & \text{otherwise} \end{cases} \tag{3}$$

Where h_{ii} represents the i-th diagonal aspect of H. therefore, we comprise $\sum_{i\in\frac{S}{P}}\|x^t\|_2 = \|HX\|_{2,1}$ Then SUnSPI form in equation (2) is written in subsequent equal form:

$$\min_{X} \frac{1}{2}\|AX - Y\|_F^2 + \lambda_S\|X\|_1 + \lambda_P\|HX\|_{2,1} + l_R + (X) \quad (4)$$

Where, $l_R + (X)$ represents the indicator purpose: $l_R + (X)$ zero if $X \geq 0$ is satisfy with $+\infty$ or else.

Then optimization trouble in equation (4) has subsequent equivalent formula:

$$\underset{U,V}{Min} \frac{1}{2}\|V_1 - Y\|_F^2 + \lambda_S\|V_2\|_1 + \lambda_P\|V_3\|_{2,1} + l_R + (V_4) \quad (5)$$

Subject to:

$V_1 = AU, V_2 = U, V_3 = HU, V_4 = U$

Where

$$V = \begin{bmatrix} V_1 \\ V_2 \\ V_3 \\ V_4 \end{bmatrix} \quad (6)$$

Assume that I represent identity matrix by appropriate size. Then it can be written equation (5) in a extra dense form:

$\min_{U,V} g(V)$

Subject to:

$$GU + BV = 0 \quad (7)$$

Where

$$g(V) \equiv \frac{1}{2}\|V_1 - Y\|_F^2 + \lambda_S\|V_2\|_1 + \lambda_P\|V_3\|_{2,1} + l_R + (V_4)$$

$$G = \begin{bmatrix} A \\ I \\ H \\ I \end{bmatrix}, B = \begin{bmatrix} -I & 0 & 0 & 0 \\ 0 & -I & 0 & 0 \\ 0 & 0 & -I & 0 \\ 0 & 0 & 0 & -I \end{bmatrix} \quad (8)$$

The ADMM algorithm for solving the problem in equation (7) is shown in Algorithm 1, where

$$l(U, V, D) \equiv g(V) + \frac{\mu}{2}\|GU + BV - D\|_F^2 \quad (9)$$

is the enlarged Lagrangian for crisis in equation (7). Here, $\mu>0$ the increased Lagrangian penalty parameter also μD denotes the Lagrange multipliers associated to constriction in GU+ BV = 0. In every iteration, ADMM algorithm consecutively reduces l to U and V, and next informs Lagrange multipliers.

By updating μ with keeping a relation among ADMM primitive enduring standard and dual remaining norm in an agreed positive period, both join to zero. Here the method make use of the KKT conditions to derive the primitive and dual residuals for the ADMM. most importantly, the primal variable should be possible, which leads to the circumstance equation:

$$GU^* + BV^* = 0 \quad (10)$$

Where U* and V*are the optimal solution of the problem in equation (7). After that, the dual variable must assure the Lagrange multiplier (or dual feasibility) form

$$0 \in \partial g(V^*) - B^T\lambda^* \tag{11}$$

$$0 = -G^T\lambda^* \tag{12}$$

Where $\partial g(V^*)$ means the sub differential of the convex purpose g at (V^*), $\lambda \equiv \mu D$ is Lagrange multipliers for the problem in equation (7).

As of the optimality state for the Step 4 of technique 1, then paper have

$$0 \in \partial g\left(V^{(k+1)}\right) + \mu B^T\left(GU^{(k+1)} + BV^{(k+1)}\right) \tag{13}$$

$$= \partial g\left(V^{(k+1)}\right) - \mu B^T D^{(k+1)} \tag{14}$$

$$= \partial g\left(V^{(k+1)}\right) - B^T\lambda^{(k+1)} \tag{15}$$

Thus, the dual optimality condition in equation (11) is satisfied by V((k+1)) and λ((k+1)) at end of the every iteration of an algorithm 1.

To meet the dual optimality condition in equation (12), the method exploit the optimality state for Step 3 of algorithm 1:

$$0 = \mu G^T\left(GU^{(k+1)} + BV^{(k)} - D^{(k)}\right) \tag{16}$$

$$= -\mu G^T D^{(k+1)} - \mu G^T B\left(V^{(k+1)} - V^{(k)}\right) \tag{17}$$

$$= -G^T\lambda^{(k+1)} - \mu G^T B\left(V^{(k+1)} - V^{(k)}\right) \tag{18}$$

Thus, after each iteration of Algorithm 1, paper have

$$\mu G^T B\left(V^{(k+1)} - V^{(k)}\right) = -G^T\lambda^{(k+1)} \tag{19}$$

Finally, the primal residual (r((k))) and dual residual (d((k))) which calculate how fine iterates of an algorithm 1 assure the KKT circumstances can described as:

$$r^{(k)} = GU^{(k)} + BV^{(k)} \tag{20}$$

$$d^{(k)} = \mu G^T B\left(V^{(k)} - V^{(k-1)}\right) \tag{21}$$

Now, the detailed SUnSPI algorithm is done by expanding the augmented Lagrangian in equation (9):

$$\begin{aligned} &l(U, V_1, V_2, V_3, V_4, D_1, D_2, D_3, D_4) \\ &= \frac{1}{2}\|V_1 - Y\|_F^2 + \lambda_S\|V_2\|_1 + \lambda_P\|V_3\|_{2,1} + l_R + (V_4) \\ &+ \frac{\mu}{2}\|AU - V_1 - D_1\|_F^2 + \frac{\mu}{2}\|U - V_2 - D_2\|_F^2 \\ &+ \frac{\mu}{2}\|HU - V_3 - D_3\|_F^2 + \frac{\mu}{2}\|U - V_4 - D_4\|_F^2 \end{aligned} \tag{22}$$

In each iteration of the ADMM scheme, sequentially minimize the function l in equation (22) to U, V_1, V_2, V_3 and V_4, next update the Lagrange multipliers. The proposed method first execute an optimization above the changeable U. By ignoring the conditions in purpose function in equation (22) that do not contain variable U, will get the reduced optimization problem as:

$$U^{(k+1)} \leftarrow \arg\min_{U} \frac{\mu}{2}\left\|AU - V_1^{(k)} - D_1^{(k)}\right\|_F^2 + \frac{\mu}{2}\left\|AU - V_2^{(k)} - D_2^{(k)}\right\|_F^2$$

$$+\frac{\mu}{2}\left\|AU - V_3^{(k)} - D_3^{(k)}\right\|_F^2 + \frac{\mu}{2}\left\|AU - V_4^{(k)} - D_4^{(k)}\right\|_F^2 \quad (23)$$

This has closed form solution:

$$U^{(k+1)} \leftarrow (A^T A + 2I + H)^{-1}[A^T(V_1^k + D_1^k + V_2^{(k)} + D_2^{(k)} + H\left(V_3^{(k)} + D_3^{(k)}\right)$$

$$+V_4^{(k)} + D_4^{(k)}] \quad (24)$$

Here the method exploit the fact that H is a diagonal matrix with diagonal elements 0 or 1, which means $H^T = H$ and $H^T H = H$.Further the values of variables V_1, V_2, V_3 and $V_4$are computed in each iteration. To update V1, the reduced optimization problem is

$$V_1^{(k+1)} \leftarrow \arg\min_{V_1} \frac{1}{2}\|V_1 - Y\|_F^2 + \frac{\mu}{2}\left\|AU^{(k)} - V_1 - D_1^{(k)}\right\|_F^2 \quad (25)$$

$$V_1^{(k+1)} \leftarrow \frac{1}{1+\mu}\left[Y + \mu\left(AU^{(k)} - D_1^{(k)}\right)\right] \quad (26)$$

Similarly, the reduced optimization problem for $V_2$is

$$V_1^{(k+1)} \leftarrow \arg\min_{V_2} \lambda_S \|V_2\|_1 + \frac{\mu}{2}\left\|U^{(k)} - V_2 - D_2^{(k)}\right\|_F^2 \quad (27)$$

whose solution represents the soft threshold:

$$V_2^{(k+1)} \leftarrow \text{soft}\left(\xi_2, \frac{\lambda_S}{\mu}\right) \quad (28)$$

Where $\xi_2 = U^{(k)} - D_2^{(k)}$ and soft $(\cdot, \tau)$ indicates the component-wise submission of the function of the soft-threshold $y \rightarrow \text{sign}(y)\max\{|y| - \tau, 0\}$.

To update V_3, the reduced optimization problem is

$$V_3^{(k+1)} \leftarrow \arg\min_{V_3} \lambda_P \|V_3\|_{2,1} + \frac{\mu}{2}\left\|HU^{(k)} - V_3 - D_3^{(k)}\right\|_F^2 \quad (29)$$

Whose solution represents a well-recognized vect-soft threshold, applied separately to every row r of inform changeable.

$$V_3^{(k+1)} \leftarrow \text{vect} - \text{soft}\left(\xi_3, \frac{\lambda_P}{\mu}\right) \quad (30)$$

Where $HU^{(k)} - D_3^{(k)}$and vect-soft $(\cdot, \tau)$ are the row-wise appliance of vect-soft-threshold purpose $y \rightarrow y\max\{\|y\|_2 - \tau, 0\}/(\max\{\|y\|_2 - \tau, 0\} + \tau)$.

To compute V_4 solve the following optimization problem

$$V_4^{(k+1)} \leftarrow \arg\min_{V_4} l_R + V_4 + \|V_3\|_{2,1} + \frac{\mu}{2}\left\|U^{(k)} - V_4 - D_4^{(k)}\right\|_F^2 \quad (31)$$

whose solution is the projection of $U^{(k)} - D_4^{(k)}$ onto the nonnegative orthant:

$$V_4^{(k+1)} \leftarrow \max\left\{U^{(k)} - D_4^{(k)}, 0\right\} \quad (32)$$

After updating U and V in each iteration, should update the Lagrange multipliers. The whole process of SUnSPI algorithm is shown in Algorithm 1.

Algorithm 1: *Pseudo code of the SUnSPI algorithm*

1. Initialization:
2. set k= 0, choose $\mu > 0, U^0, V_1^0, V_2^0, V_3^0, V_4^0, D_1^0, D_2^0, D_3^0, D_4^0$
3. repeat:
4. Compute $U^{(k+1)}$ via Eq. (24)
5. Compute $V_1^{(k+1)}$ via Eq. (26)
6. Compute $V_2^{(k+1)}$ via Eq. (28)
7. Compute $V_3^{(k+1)}$ via Eq. (30)
8. Compute $V_4^{(k+1)}$ via Eq. (32)
9. $D_1^{(k+1)} \leftarrow D_1^{(k)} - AU^{(k+1)} + V_1^{(k+1)}$
10. $D_2^{(k+1)} \leftarrow D_2^{(k)} - U^{(k+1)} + V_2^{(k+1)}$
11. $D_3^{(k+1)} \leftarrow D_3^{(k)} - HU^{(k+1)} + V_3^{(k+1)}$
12. $D_4^{(k+1)} \leftarrow D_4^{(k)} - U^{(k+1)} + V_4^{(k+1)}$
13. Update iteration: $k \leftarrow k + 1$
14. Until some stopping criterion is satisfied.

The obtained results from Unmixing method are then processed using the clustering algorithm for the better classification of the materials present in the hyper-spectral images.

3.2. Adaptively Regularized Kernel-Based Fuzzy C-Means

An adaptively regularized kernel-based fuzzy C-means clustering framework is proposed for the segmentation of materials present in the mars images. The framework can be worked on the three bases in which the local standard grayscale individual restored through the grayscale of the median filter, average filter and devised slanted images correspondingly. The techniques are employed for the heterogeneity of grayscales in neighborhood. Further, it is evaluated for restricted contextual information and restores the measure Euclidean distance by Gaussian radial basis kernel function. The compensation of algorithm is adaptiveness to restricted context, improved robustness to protect image particulars, self-government of clustering parameter, and reduced computational expenses.

In proposed frame work the adaptively regularized kernel-based FCM framework is denoted as ARKFCM. In this method, calculation of the adaptive regularization parameters φ_i are associated with every pixel to control the contextual information. The objective function is defined in equation (33).

$$J_{ARKFCM} = 2\left[\sum_{i=1}^{N}\sum_{j=1}^{c} u_{ij}^{m}\left(1 - K(x_i, v_j)\right) + \sum_{i=1}^{N}\sum_{j=1}^{c} \varphi_i u_{ij}^{m}\left(1 - K\left(\overline{x_i}, v_j\right)\right)\right] \quad (33)$$

The minimization of JARKFCM (u,v) can be calculated through an alternate optimization procedure using equations (34) and (35)

$$u_{ij} = \frac{\left(\left(1 - K(x_i, v_j)\right) + \varphi_i \left(1 - K(\overline{x_l}, v_j)\right)\right)^{-1/(m-1)}}{\sum_{k=1}^{c} \left(\left(1 - K(x_i, v_k)\right) + \varphi_i \left(1 - K(\overline{x_l}, v_k)\right)\right)^{-1/(m-1)}} \quad (34)$$

$$v_j = \frac{\sum_{i=1}^{N} u_{ij}^{m} \left(K(x_i, v_j) x_i + \varphi_i K(\overline{x_l}, v_j) \overline{x_l}\right)}{\sum_{i=1}^{N} u_{ij}^{m} \left(K(x_i, v_j) + \varphi_i K(\overline{x_l}, v_j)\right)} \quad (35)$$

When $\bar{x}$ is replaced with the grayscale of the average/median filter of the original image, then the algorithm is denoted as $ARKFCM_1/ARKFCM_2$. When $\overline{x_l}$ is replaced with the weighted image $\overline{\xi_l}$, then the algorithm is denoted as $ARKFCM_w$.

The main steps for the proposed method is described in algorithm 2.

Algorithm 2: *Steps involved in the Proposed Method*

1. Initialize threshold ε = 0.001, m = 2, loop counter t=0, v, and $u^{(0)}$.
2. Calculate the adaptive regularization parameter φ_i.
3. Calculate $\overline{x_l}$ for $ARKFCM_1$ *and* $ARKFCM_2$ or ξ_i for $ARKFCM_w$.
4. Calculate cluster canters $v_j^{(t)}$ and$u^{(t)}$.
5. Calculate the membership function u^{t+1}.
6. If max $\left\|u^{(t+1)} - u^{(t)}\right\| < \varepsilon$ or t > 100 then stop; otherwise, update t=t+1 and go to step (4).

3.3. Segmentation using Watershed Algorithm

The clustered image of mars hsv000f9c0_01_ra2095_trr3 is chosen in such a way that it should contain the more information about the material. Further the clustered images are processed with the Watershed segmentation algorithm in which the differentiation of the materials is done.

Let $u(x, y)$ with $(x, y) \in R^2$, be a scalar function recitation an image I. Then, morphological of gradient of I is,

$$\delta_D u = (u \oplus D) - (u \ominus D) \quad (36)$$

where $(u \oplus D)$ and $(u \ominus D)$ are the elementary dilation and erosion of u respectively by the formation part D. The morphological Laplacian specified by

$$\Delta_D u = (u \oplus D) - 2u + (u \ominus D) \quad (37)$$

In morphological Laplacian,it permits us to differentiate authority zones of minima and suprema: areas with $\Delta_D u < 0$ are measured as pressure zones of suprema, though areas by $\Delta_D u > 0$ are influence zones of minima. Then $\Delta_D u = 0$ permits us to understand edge location, and signify necessary assets for structure of morphological filter. The essential

design is to relate dilation or erosion to an image I, depending on either the pixel can be located in the pressure zone of the maximum or a minimum.

3.4. Singular Spectrum Analysis

The output of the Watershed Segmentation algorithm of an image hsv000f9c0_01_ra2095_trr3 is given for the Feature extraction. Further in that the extraction of features from these Hyperspectral images is done using Singular Spectrum Analysis approach. By eliminating noise component in extorting the quality of mars dataset, the discerning capability of characteristics will be enhanced significantly. Singular spectrum analysis aspire to provide enhanced renovation of spectral pixel in Hyperspectral imaging, by resources of major Eigen value components[21] while reducing the noisy components. Feature extraction by singular spectrum analysis approach for mars dataset results in better classification.

3.5. Adaptive Resonance Theory (ART) Classifier

The ART Classifier is used for the better classification of the hyper spectral images of Mars dataset, where it uses the unlabelled instances similar to any other decision list classifier. Initially a specified instance can be checked sequentially beside each rule until and unless an identical rule can be obtained. Eventually any instance would arrive at the matching rule possibly when counting a incurable default rule. Further the matching rule can considered with mainly general class that can establish in training information. The unacceptable values are mechanically sent to another class. When the algorithm classifies the data for some attributes with unknown values, a different method could be followed. For the unavailability of associated rules, ART classifier will end up in a default class value for respected mars image. The most awful case is when the association rules cover every examples in input dataset for building the list, a specified case could direct to nowhere in decision list. That instance would be considered with most general class in training information covered by the current sub-list in this improbable, but possible case for an image hsv000f9c0_01_ra2095_trr3.

Resonance Theory for the mars dataset represents the scalable and competent values. When there is a large dataset, the ART classifier will give the better accuracy when compared to other classifier. Seamlessly they can handle primary keys in the input data as well as noise. For the organization rule, mining methods entangled in ART provide an easy and effectual device to undertake a broad assortment of circumstances. Further it doesn't require of using more precise, compound and artificial methods to resolve every trouble that occurs in the classification of mars dataset. ART simultaneously, determines the several rules. Besides, ART do not suffer as of the I/O blockage familiar to option rule and decision of the list inducer, because it uses a competent association rule mining method to produce hypothesis. Therefore, in this paper specially for mars dataset the ART represents appropriate for the handling massive dataset typically establish in the real-world struggles.

4. Experimentation

The performance of the proposed system is tested with real time image of mars dataset, which has been taken from OMEGA instrument. The OMEGA instrument is capable to build up a map of surface composition. The given input image of OMEGA mars dataset is shown in Figure 3. The proposed system contains two phases called testing and training. A pre-processing method based on singular value decomposition (SVD) algorithm is considered for the query image hsv000f9c0_01_ra2095_trr3.

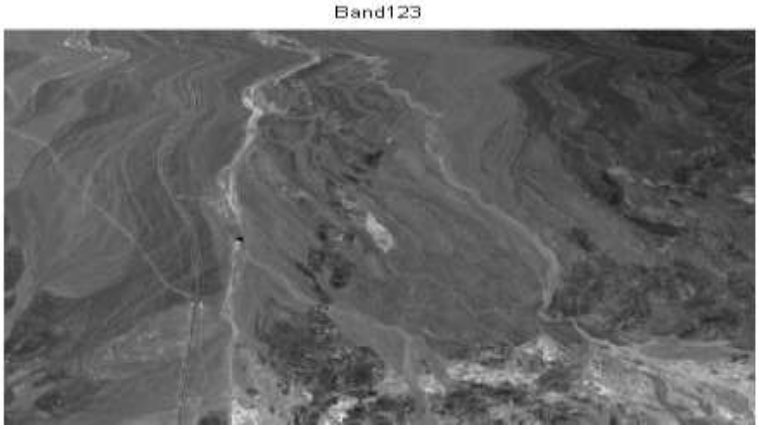

Figure 3. Input Hyperspectral Image

Further Unmixing algorithm termed "Sparse Unmixing of Hyperspectral Data Using Spectral a Priori Information[22]" with the Singular Spectrum Analysis approach is applied on the above mentioned mars image. which yields to get the better result for the Clustering by "Adaptively Regularized Kernel-Based Fuzzy C-Means[23]" and Segmentation by "Watershed" algorithm. The resultant segmented images of an mars image hsv000f9c0_01_ra2095_trr3 are shown in Figure 4.

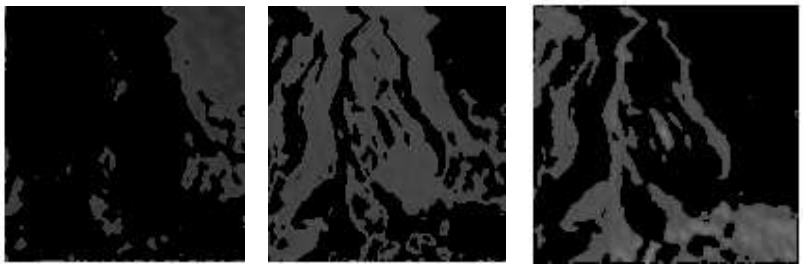

Figure 4. Segmented Output of the Input Image

The Feature extraction is done using singular spectrum analysis approach. These features are matched with knowledge base containing the ground truth values using ART Classifier. Series of real time neural network models such as ART provides both unsupervised and supervised learning, prediction and detection, mainly with pattern recognition for mars dataset. Thus in the proposed system the resultant classified mineral output images of an image hsv000f9c0_01_ra2095_trr3 are obtained and presented in Figure 5. Further the respective classified output is shown in Figure 6.

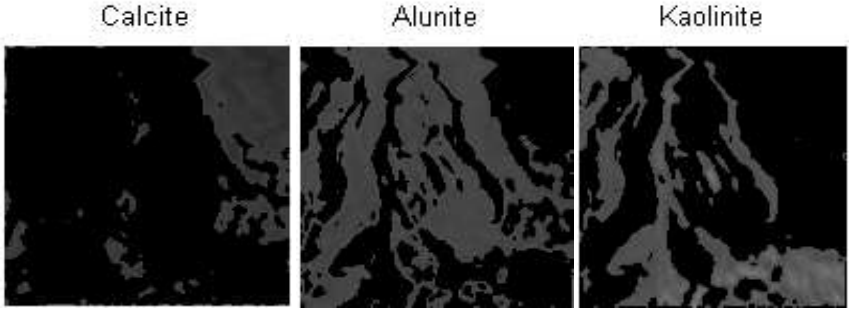

Figure 5. Segmented Output of (a) Calcite (b) Alunite (c) Kaolinite

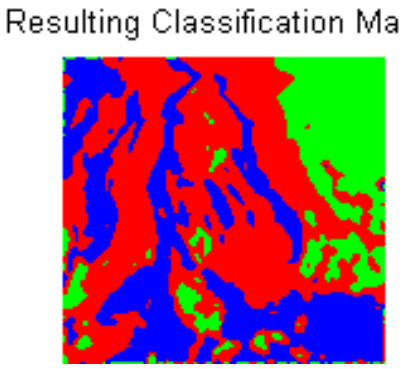

Figure 6. Classification Output Map

By employing ART classifier the three different minerals are effectively identified and categorized for OMEGA mars dataset(hsv000f9c0_01_ra2095_trr3). The performance of the proposed method is compared with other two methods viz. k-means and SMLR and PSO and pictorially depicted in Figure 7.

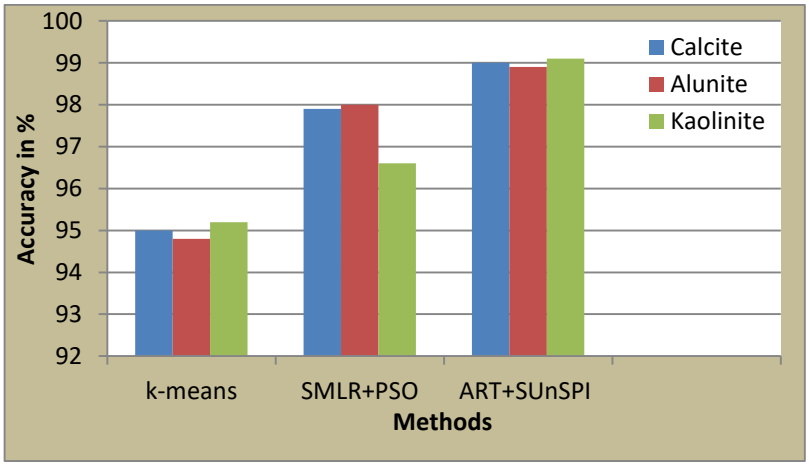

Figure 7. Comparison of the Proposed Work with other Related Works

The concert evaluation of proposed method and previous methods viz. k-means[11] clustering and segmentation, SMLR and PSO method[18] is shown in Figure 7. The results demonstrate that the proposed hyperspectral image classification and unmixing by using ART and SUnSPI Techniques for OMEGA Mars dataset gives better result. In future the proposed method can be extended to find the percentage of the mineral content present on the surface of the Mars data collected from the different instruments.

5. Conclusion

The proposed method presented novel algorithms for Unmixing with classification of Hyperspectral images. For pre-processing the Hyperspectral data, singular value decomposition (SVD) algorithm is employed. A new algorithm term SUnSPI is used for the Unmixing of Hyperspectral information. Further the output of SUnSPI is clustered by using "Adaptively Regularized Kernel-Based Fuzzy C-Means". The clustered images are then segmented using the Watershed algorithm. Further the segmented images are employed for the feature extraction. The feature vector extracted from singular spectrum analysis is matched with features vectors stored in the knowledge base using ART Classifier. In ART classifier the input patterns is utilized for better level of classification. This method is exposed to offer accurate classification of hyper-spectral descriptions in

both spectral and spatial field in short span of time. Further the proposed method can be experimented with statistical techniques for better identification/classification of minerals of hyper spectral images. The percentage of the mineral content present on the surface of the Mars data from the different dataset can be computed by extending the proposed technique.

References

[1] O. Eches, N. Dobigeon and J.-Y. Tourneret, "Enhancing Hyperspectral Image Unmixing with Spatial Correlations", IEEE Transactions on Geoscience and Remote Sensing, vol. 49, no. 11, **(2012)**, pp. 4239 -4247.
[2] S. Mei, Q. Bi, J. Ji, J. Hou and Q. Du, "Spectral Variation Alleviation by Low-Rank Matrix Approximation for Hyperspectral Image Analysis", IEEE Geoscience and Remote Sensing Letters, vol. 13, no. 6, **(2016)**.
[3] P. V. Giampouras, K. E. Themelis, A. A. Rontogiannis and K. D. Koutroumbas "Simultaneously Sparse and Low-Rank Abundance Matrix Estimation for Hyperspectral Image Unmixing", IEEE Transactions on Geoscience and Remote Sensing, vol. 54, no. 8, **(2016)**, pp. 4775-4789.
[4] X. Xu, X. Tong, A. Plaza, Y. Zhong, H. Xie and L. Zhang, "Using Linear Spectral Unmixing for Subpixel Mapping of Hyperspectral Imagery: A Quantitative Assessment", IEEE Journal of Selected Topics in Applied Earth Observations and Remote Sensing, vol. 10, no. 4, **(2017)**, pp. 1589-1600.
[5] R. P. Karchi and Nagesh B.K, "A Review of Spectral Unmixing Algorithms in the context of Mars Dataset", International Journal of Latest Trends in Engineering and Technology (IJLTET), 2013, ISSN: 2278-621X, Special Issue-IDEAS-2013, **(2013)**, pp. 55-60.
[6] S. Liu, L. Bruzzone, F. Bovolo and P. Du, "Unsupervised Multitemporal Spectral Unmixing For Detecting Multiple Changes In Hyperspectral Images", IEEE Transactions on Geoscience and Remote Sensing, vol. 54, no. 5, **(2016)**, pp. 2733-2748.
[7] A. Zare and K. C. Ho, "Endmember Variability in Hyperspectral Analysis: Addressing Spectral Variability During Spectral Unmixing", IEEE Signal Processing Magazine, vol. 31, no. 1, **(2014)**, pp. 95-104.
[8] Y. Altmann, M. Pereyra and J. Bioucas-Dias, "Collaborative Parse Regression Using Spatially Correlated Supports-Application to Hyperspectral Unmixing", IEEE Transactions on Image Processing, vol. 24, no. 12, **(2015)**, pp. 5800-5811.
[9] R. Feng, Y. Zhong, X. Xu and L. Zhang, "Adaptive Sparse Subpixel Mapping With a Total Variation Model for Remote Sensing Imagery", IEEE Transactions on Geoscience and Remote Sensing, vol. 54, no. 5, **(2016)**, pp. 2855-2872.
[10] Y. Gu, Y. Zhang and J. Zhang, "Integration of Spatial–Spectral Information for Resolution Enhancement in Hyperspectral Images", IEEE Transactions on Geoscience and Remote Sensing, vol. 46, no. 5, **(2008)**, pp. 1347-1358.
[11] F. Kowkabi, H. Ghassemian and A. Keshavarz, "Enhancing Hyperspectral Endmember Extraction Using Clustering and Oversegmentation-Based Preprocessing", IEEE Journal of Selected Topics in Applied Earth Observations and Remote Sensing, vol. 9, no. 6, **(2016)**, pp. 2400-2413.
[12] S. Zhang, J. Li, J. Plaza, H.-C. Li and A. Plaza, "Spatial weighted sparse regression for hyperspectral image unmixing", IEEE International Geoscience and Remote Sensing Symposium (IGARSS), **(2017)**, pp. 225-228.
[13] Y. Altmann, M. Pereyra and J. Bioucas Dias, "Linear spectral unmixing using collaborative sparse regression and correlated supports", Seventh Workshop on Hyperspectral Image and Signal Processing: Evolution in Remote Sensing (WHISPERS), **(2015)**, pp. 1-4.
[14] M. Nie, Z. Liu, H. Xu, X. Xiao, F. Su, J. Chang and X. Li, "Hyperspectral Image Unmixing for Classification and Recognition: An Overview", International Journal of Signal Processing, Image Processing and Pattern Recognition, vol. 8, no. 12, **(2015)**, pp. 223-236.
[15] M. Nagarajan and S. Vasudevan, "A Basic Study of Image Processing and Its Application Areas", International Journal of Engineering Research and Technology, vol. 6, no. 7, **(2017)**, pp. 343-348.
[16] S. Lal and R. Kumar, "Enhancement of Hyperspectral Real World Images Using Hybrid Domain Approach", International Journal of Image, Graphics and Signal Processing, vol. 5, **(2013)**, pp. 29-39.
[17] M. Nagarajan and S. Karthikeyan, "A New Approach to Increase the Life Time and Efficiency of Wireless Sensor Network", IEEE International Conference on Pattern Recognition, Informatics and Medical Engineering (PRIME), **(2012)**, pp. 231-235.
[18] R. P. Karchi and B. K. Nagesh, "A Hybrid Approach for Hyper Spectral Image Segmentation Using SMLR and PSO Optimization", Proceedings of Recent Trends in Image Processing and Pattern Recognition, Springer Nature Singapore, CCIS 709, **(2017)**, pp. 1-9.
[19] M. Ezhilarasi and V. Krishnaveni, "An Optimal Solution To Minimize The Energy Consumption in Wireless Sensor Networks", International Journal of Pure and Applied Mathematics, vol. 119, no. 10, **(2018)**, pp. 829-844.

[20] S. A. El_Rahman, W. A. Aliady and N. I. Alrashed, "Supervised Classification Approaches to Analyze Hyperspectral Dataset", International Journal of Image, Graphics and Signal Processing, vol. 5, **(2015)**, pp. 42-48.
[21] S. A. Angadi and S. M. Hatture, "Hand Geometry Based User Identification Using Minimal Edge Connected Hand Image Graph", IET Computer Vision (ISSN: 1751-9632), **(2018)**, pp. 1-9.
[22] A. Mohammed Rufai, G. Anbarjafari and H. Demirel, "Lossy Image Co[mpression Using Singular Value Decomposition and Wavelet Difference Reduction", Digital Signal Processing, vol. 24, **(2014)**, pp. 117-123.
[23] A. Elazab, C. Wang, F. Jia, J.-H. Wu, G. Li and Q. Hu, "Segmentation of Brain Tissues from Magnetic Resonance Images Using Adaptively Regularized Kernel-Based Fuzzy C-Means Clustering", Computational and Mathematical Methods in Medicine, vol. 2015, Article ID 485495, **(2015)**, pp. 1-12.

Authors

Rashmi P. Karchi, received her Bachelor's Degree in Computer Science from Karnatak University, Dharwad, Karnataka State, India, M.Sc in Statistics from Karnatak University, Dharwad, Karnataka State, India. M.Tech degree in Computer Cognition and Technology from Mysore University, Mysuru, Karnataka State, India, and currently pursuing her Ph.D in Computer Science from Bharathiar University, Coimbatore, Tamilnadu, India. Her areas of interest are Biometrics, Image processing, Signal Processing, Remote Sensing, Hyperspectral Image Analysis and Statistics.

Dr. Nagarajan Munusamy is currently Associate Professor in Computer Applications Department, CMS College of Science & Commerce, Tamilnadu, India. He has completed Ph.D in Computer Science in 2012. He has published many reputed International Journals and has an experience more than 15 years in the Industry and Academic. His research area includes Wireless Sensor Networks, Remote Sensing, Image Processing and Network Security.

